HF Coastal Ocean Radar in an Observing System

M. L. Heron[1], P.V. Ridd[1], D.J.M. Greenslade[2], W.J. Skirving[3] and S.F. Heron[3]

[1]AIMS@JCU, Marine Geophysical Laboratory, James Cook University, Townsville, QLD 4811
[2]Bureau of Meteorology Research Centre, GPO Box 1289, Melbourne, VIC 3001
[3]Coral Reef Watch, NOAA/NESDIS, Maryland, USA

Abstract
The HF coastal ocean radar in the southern part of the Great Barrier Reef is part of a national integrated marine observing system, and the data will be available for research applications from a national archive. The primary archived product is hourly values of surface current vectors, significant wave heights and wind directions at over 1000 grid points at 4 km spacing over the shelf and adjacent ocean. A review of currently associated research projects includes validation of hydrodynamic modelling, tsunami detection, connectivity of reefs and islands, empirical physical process modeling, and combining radar surface current data with satellite-based sea surface temperature data to produce an index of mixing in the vertical column of water.

1 Introduction

The global trend towards integrated ocean observing systems is rapidly spreading within the marine science community in Australia with the roll-out of the National Collaborative Research Infrastructure Strategy (NCRIS), and within that, the Integrated Marine Observing System (IMOS). One of the elements of IMOS is the Australian Coastal Ocean Radar Network. The first element of ACORN is the installation of a dual station phased array radar system in the southern part of the Great Barrier Reef.

2. HF Ocean Radar

Coastal ocean surface radar is a land-based technique which uses scattering from the rough sea surface to obtain echoes which are Doppler shifted by the dynamics of the sea. It has been shown (Crombie, 1955) that the scatter is predominantly a Bragg interaction between the radio wave and the sea surface gravity wave that is propagating in the same direction and with half the wavelength of the radio wave. This Bragg interaction gives two strong first-order lines in the echo spectrum; one from the resonant gravity wave moving radially away from the station, and one from the resonant gravity wave moving towards the station. The Doppler shifts of these lines in still water are related to the deep water gravity wave dispersion

$$c = \sqrt{g/k} \qquad (1)$$

where k is the wavenumber of the gravity waves and g is the gravitational acceleration. If there is a bulk movement of the sea water (current) with a component in the radial direction from the station, then this is manifest as additional Doppler shift and the observed Doppler shifted frequencies for the two first-order lines are

$$f_D = \pm\sqrt{\frac{g}{2\pi\lambda}} - \frac{v_r}{\lambda} \qquad (2)$$

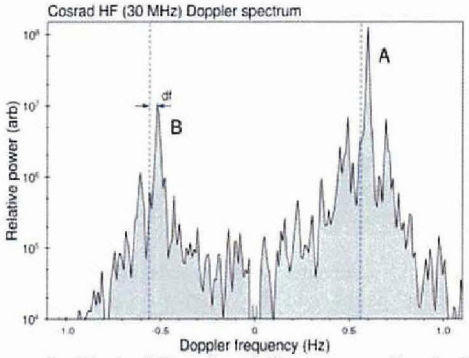

Figure 1. Typical Doppler shift spectrum for the JCU 30 MHz COSRAD radar showing strong first-order lines with sidebands of second-order energy. The vertical dashed lines mark the position of the lines for still water, and the interval df is the Doppler shift due to the radial component of the surface current.

where λ is the wavelength of the sea surface gravity wave, and v_r is the radial component of the surface current (positive outwards).

The first-order spectral lines are generally more than 30 db above the noise in the band, as shown in Fig. 1, and are generally more than 10 db above the second-order echo energy which arises from double scatter processes (Barrick, 1972). The identification of the peaks and calculation of their frequencies is therefore amenable to automation with a good robustness and reliability. In a monitoring situation each station would normally run for about 5 minutes to produce time series from which energy spectra may be calculated.

If each radar station can locate the radial distance and the azimuth of each echo pixel over a large area to be mapped, then the radial components of surface currents can be combined to find the vector at each position. The area covered by the GBR coastal ocean radar is shown in Fig. 2. Each station can record radial currents in about a 60^{O} sector of azimuth and 150 km in range. The shaded area is where the radial

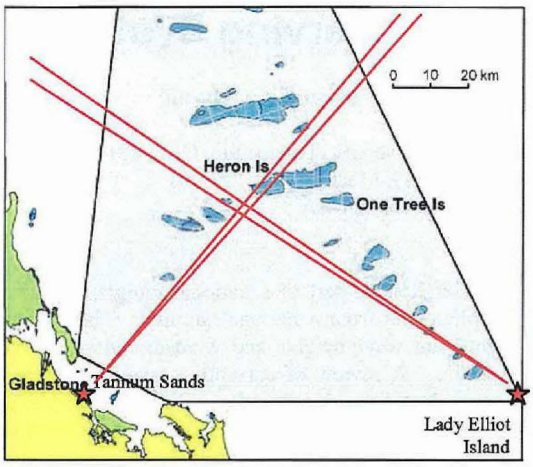

Figure 2. The configuration of the GBR coastal ocean radar with the Tannum Sands station at the bottom left and the Lady Elliot Island. station on the bottom right. The shaded area indicates the primary grid of points for which data are produced.

component data from the stations overlap so that one can calculate surface current vectors. The radar beams are approximately orthogonal near Heron Island.

The second-order energy in the side-bands around the first-order peaks can be used to determine wave parameters. With very 'clean' spectra where the second-order energy is more than 10 db above the noise, it is possible to carry out an inversion analysis to find the directional wave spectrum (Wyatt, 1988; Wyatt and Holden, 1994). As a general rule, the full directional wave spectrum analysis can be done for pixels out to about half the range to which surface current vectors can be extracted. A more robust analysis is available for significant wave heights, and this can be used routinely at individual pixels across a similar mapped area to surface currents (Barrick, 1977; Graber and Heron, 1997; Heron and Heron, 1998, Heron and Prytz, 2002). This algorithm relies on the ratio of energy in the second-order to first-order bands of the Doppler spectra.

3. The GBR Coastal Ocean Radar

The layout of the GBR coastal ocean radar is shown in Fig.2. At each site we have a WERA phased array radar which operates at 8.348 MHz with an available bandwidth of 33.4 KHz and vertical polarisation. The receiver antennas form a conventional 16-element array, spaced half a wavelength (17.97 m) apart with each one having its own coaxial cable back to its own receiver in the Radar Shack. By adding and subtracting phase delays the array can be used to form a beam, at a post-analysis stage, on any point in the mapped field. The combination of aperture and bandwidth enables us to mark out a grid of points 4 km apart over the shaded area of Fig. 2 for data production; about 750 grid points.

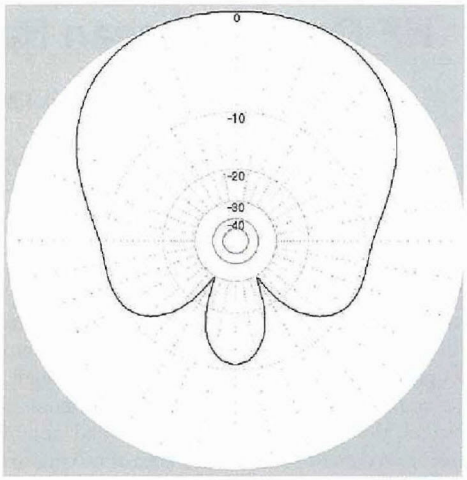

Figure 3. The polar pattern of the transmit array is designed to give a broad lobe in the forward (up the page) direction; have a high front-to-back ratio; and a reduced lobe in the direction of the receive array of antennas. The scale is in db. (provided by Helzel Messtechnik GmbH)

Four vertical antenna elements form the transmitter array. The four elements are set at the corners of a rectangle in such a way as to radiate into the oceanic half-space from the shore; to maximize the front-to-back ratio; and to cast a null in the direction of the receive array of antennas. The design polar pattern of the transmit array is shown in Fig. 3.

In their routine mode of operation, the radar sites are alternately 5 minutes on and 5 minutes off. The main reason for this is that they use the same operating frequency. The choice of 5 minutes is an optimization between capturing fast events (like in the monitoring of tsunamis) and accuracy of the determination of radial currents from the time series. For the latter, the shorter the time series the broader are the first-order spectral lines. This is shown in Fig. 4 where the operating frequency has been stepped from 5 to 30 MHz in 5 MHz intervals, except for the dashed line which is at 8.348 MHz. For 5 minute time series the error in the radial surface current is about ± 7 cm/s. Note that any windowing in the time series analysis makes the accuracy worse.

The maintenance of these radar stations remote from the base at James Cook University in Townsville presents a challenge. The data stream comes by phone every 10 minutes. Each transmitted file includes performance data from each of the 12 receive antennas, from the transmitter, and also status indicators for each part of the system at the field site. Data from environmental sensors (temperature, humidity, wind) are included in the 10-minute data packets. The maintenance plan depends upon diagnosis of faults based on the information arriving at the central laboratory. Remediation is done by a local

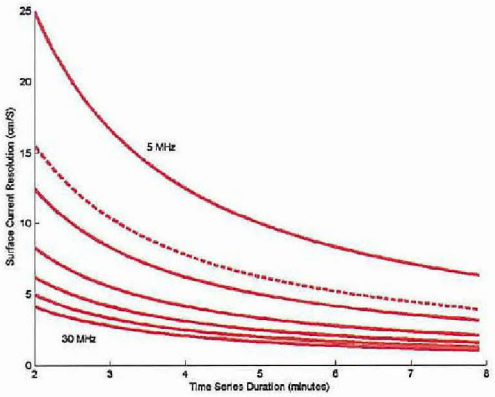

Figure 4. The accuracy of determining the radial current component depends on the length of the time series from which the Doppler spectrum is produced, and the radar operating frequency.

technician at the site, or by someone travelling with a toolbox from the centre.

At the basic 5-minute intervals the spectra are analysed in the on-site computer and by phone line the following data are transmitted to a central laboratory at James Cook University for each grid point:

- Radial component of velocity;
- Ratio of first to second-order energy;
- Ratio of first-order peak energies (A to B in Fig. 1)

At the central laboratory data will be combined from the two stations to produce every 10 minutes:

- Maps of surface current vectors at the grid points;
- Significant wave heights at the grid points;
- Wind direction at the grid points.

This is the 10-minute near real-time archive.

At each station the individual spectra are incoherently averaged over 1 hour. This is a non-linear process and it is not the same to derive parameters from six spectra and average them, as it is to incoherently average the spectra and then do the parameter extraction analysis. At hourly intervals the incoherently averaged spectra are analysed and by phone, the following data are transferred to the laboratory:

- Radial component of velocity;
- Ratio of first to second-order energy;
- Ratio of first-order peak energies.

At the central laboratory data will be combined from the two stations to produce every hour:

- Maps of surface current vectors at the grid points;
- Significant wave heights at the grid points;
- Wind direction at the grid points.

This is the hourly near real-time archive.

At two-hourly intervals the Doppler spectra are spatially smoothed over 4 x 4 pixels and temporally smoothed over the 2 hours. These smoothed spectra on the coarse spatial grid will be sent over the phone to the central laboratory where they will be analysed together with the complementary spectra from the other station, to provide directional wave spectra at the coarse grid points.
This is the two-hourly near real-time archive.

Another level of archiving is to store the 'raw' spectra for every grid point every 10 minutes. This is too much data to send by phone line and will be stored on hard media at the radar stations and freighted monthly to the central laboratory for archiving.

Protocols are being developed for the quality assurance of archived data, and for the provision of metadata in the archived files under the principles of the Integrated Marine Observing Strategy (IMOS) which aims to provide easy and free access.

4. Applications of the Data

There are several projects that have specifically registered interest in using the data from the GBR coastal ocean radar. One of the reasons for placing the GBR radar over the Capricorn/Bunker Groups was to recognize the international coral bleaching project being carried out in that area, and to enable collaboration with the participating institutions.

4.1 Hydrodynamic Modelling

In an Australian Research Council Industry Linkage project on biological responses to coral bleaching a high-resolution 3-dimensional hydrodynamic model is being developed for the Capricorn Group. The hourly surface current values from the radar on the 4 km grid will provide a useful validation for the model. There is potential here to extend this work to evaluate the assimilation of ocean surface radar data into the hydrodymanic model to run a now-casting product.

4.2 Connectivity between reefs and islands.

In the Great Barrier Reef the destructive events in recent decades have been crown of thorns starfish plagues, tropical cyclones and coral bleaching. After a destructive event, success of recolonisation by coral planulae (larvae) depends critically on the distance from neighbouring reefs and the pattern of ocean currents in the intervening space (Sammarco, 1994). Previous work has been based on hydrodynamic modelling. Work by Sammarco and Andrews, 1988, 1989) showed that trapped eddies on the leeward side of Helix Reef on the GBR had the effect of retaining larvae and helping to self-seed the reef. Recent work by Gerlach et al, 2007 showed a biological driver for self-seeding for larvae with a swimming (and olfactory) capability.

The hourly data from the radar grid points can be used in a psuedo-Lagrangian calculation for the tracks of

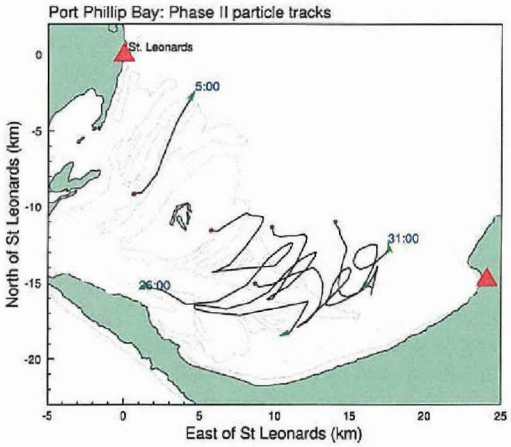

Fig 4. Psuedo-Lagrangian tracks in Port Phillip Bay. The shaded area is land and the triangles indicate the location of the radars at St Leonards and Safety Beach. The solid lines are the tracks with a dot to mark the release point and a number at the other end to show the number of hours the particle was tracked before it went off the mapped area. For larvae simulations and diffusion studies we use close-spaced release points.

parcels of surface water (Prytz and Heron, 1999, see Fig.4). At a given starting time and position the data are interpolated for the surface current; the parcel of water is then stepped along at that velocity for 1 hour to a new point; and so on until the data record ends or the parcel runs off the mapped area. In this project the advection hypothesis is used with the time and space maps of surface currents from the HF Ocean Radar to identify the connectivity paths over a two-year data set. By releasing drifters at points more closely spaced than the radar grid, the error in the pseudo-Lagrangian calculation due to the filtering out of sub-grid scale currents is evaluated. This work will also produce results on horizontal diffusion in the GBR Lagoon.

4.3 Empirical Physical Process Modelling

Mao et al. (2007) assume that surface currents from an HF radar, at each point on the sea surface can be represented as a linear superposition of basis elements which are related to the physical driving effects. The relevant matrix of coefficients can be evaluated from historical data at each grid point to form a basis for synthesizing the surface current at any time that the driving parameters are available. This Empirical Physical Process Model was demonstrated in Bass Strait. For each grid point on the radar map, a conventional tidal components analysis was done and the tide removed from the record. The residuals were clearly correlated with wind, but they found that the coefficients depended on the wind speed and wave age. The total response of surface current to wind is a result of both momentum transfer by wind shear stress and Stokes drift generated by waves. Under different fetch conditions, the difference in sea state results in a difference in the Stokes drift. This is a new and somewhat controversial result which will be confirmed in the GBR region where longer data runs with more varied conditions will be available. This approach offers a new and powerful approach to nowcasting and forecasting of surface currents for operational purposes.

4.4. Coral Bleaching and Dynamical Thermal Capacitance

In this project the methodology for producing maps of an index for dynamical thermal capacitance (DTC) from the surface current and wave height data produced by the HF Ocean Radar is being developed. The concept of DTC of coastal ocean was introduced by Skirving et al. (2006) by considering that a stratified ocean will absorb solar radiation into the uppermost layer and cause a rise in temperature. If the ocean is vertically mixed then any solar radiation will have to heat the whole water column - the result is that for a given input of heat energy, the surface temperature increase is less than what it would be in a stratified ocean. The new concept of DTC therefore is derived from mixing and serves as an index for the potential of the ocean's surface temperature to rise and threaten to produce coral bleaching.

The challenge here is to estimate the vertical profile of density using the measured surface current speed and significant wave height, and accurate bathymetry. The approach will be to solve the energy balance between turbulent kinetic energy produced by the current and the mixing by waves and wind-induced turbulence, and the insolation. The effective DTC for insolation depends on the net energy balance. At the extremes, if there is no mixing then the insolation energy is stored in a thin (stratified) layer with low DTC; if the mixing is intense, then the insolation energy is stored in the entire water column and the DTC is high.

We make the common assumption of a linear model for the vertical eddy viscosity given by $N_z = k u_* z$, which leads to the familiar logarithmic bottom friction layer

$$u = \frac{u_*}{k} \ln\left(\frac{z}{z_O}\right), \qquad (3)$$

where u is speed, u_* is the stress velocity, z is the depth, and z_0 is the thickness of the friction layer. Adopting the approach by Simpson and Hunter (1974) (also used by many others e.g. Hearn, 1985; de Silva Samarasinghe, 1989) we can write the total kinetic energy in the layer as

$$TKE = \overline{\rho} \int_0^h N_z \left(\frac{\partial u}{\partial z}\right)^2 dz \ , \qquad (4)$$

where $\overline{\rho}$ is the column-averaged density. A coefficient α is used to establish a rate of mixing energy that can be provided by the currents. The mixing power available from the current is then

$$P_c = -\alpha (TKE) \ . \qquad (5)$$

Previous research has indicated that $\alpha = 0.037\ s^{-1}$.

It has recently been shown that the wind-induced surface current depends on wind speed, wave height and the state of development of the sea state (Mao and Heron, 2007) With this driving energy a boundary layer can be constructed from the surface down, to estimate mixing. The wave energy available for mixing comes from an estimate of the amount of wave energy that is lost to turbulence.

The data available for calculating this energy balance are surface currents and wave heights from the radar, and wind speed from anemometers on available island sites. Calibration of the coefficients and validation of the DTC calculation are coming from *in situ* measurements of temperature profiles using thermistor strings and a Slocum Glider.

The Dynamical Thermal Capacity is a new concept and is inspired by the success of the Degree Heating Week (DHW) index produced by the Coral Reef Watch group within the National Oceanic and Atmospheric Administration (Arzayus and Skirving, 2004). The DHW global index is produced two times per week by NOAA from satellite data, and is used by many coral reef management authorities around the world. The new DTC index will be on a finer scale (4 km grid points compared with 50 km) than the DHW index and will be a useful refinement. It will indicate which reefs within a group are more susceptible to bleaching This is a completely new concept which will make a significant contribution to monitoring and managing coral bleaching.

4.5 The Detection of Tsunamis by HF Radar

Tsunamis are long wavelength, long period gravity waves which are normally produced by earthquakes or underwater slumps. The wave period of tsunamis depends upon the scale size of the bathymetric event and water depth. Historical records of impacts on the shore indicate that the tsunami wave period (the so-called tsunami window) is in the range 5-30 minutes (Bryant, 2001). The connection between earthquakes and tsunamis is not well understood; some marine earthquakes do not produce tsunamis, and some tsunamis occur with quite small seismic activity. Once the pulse of elevated water is produced it can travel large distances with little attenuation and some dispersion. The elevation of the tsunami waves in the open ocean is generally less than about 0.5 m. This is amplified to tens of metres at the shore and can produce run-up of over 100 m (Bryant, 2001).

The tsunami on 26 December 2004 produced wave height at the beach of the order of 10 m and the open ocean elevation was 0.5 m as measured by the JASON 1 altimeter (Smith et al., 2005) in the Indian Ocean some 2 h after the earthquake in the Sumatra - Andaman Islands.

Barrick (1979) showed that HF radars have the potential to observe tsunamis up to 80 km offshore. More recently there has been a move towards HF radars with longer ranges to map surface currents to ranges of up to 200 km, and the installation in the southern Great Barrier Reef has the capability of mapping beyond the edge of the continental shelf. Barrick's concept was to observe the pattern of tsunami wave crests and troughs as the parallel wave-fronts propagate across the shelf towards the coast. In this project we build on that concept to evaluate the feasibility of operational long-range HF radars to detect tsunami effects at the edge of continental shelves. Here we have the advantage of amplification of surface currents as the tsunami encounters the shelf edge, but the challenge is in the use of long-range HF radar systems where time resolution is often sacrificed.

When a tsunami wave crest encounters the steep bathymetry gradients at the edge of the continental shelf the waves become non-linear and the surface currents are amplified differently at different points depending on the local bathymetry. Numerical modelling can determine the expected amplification from a range of simulated tsunami origins and amplitudes. This will provide a spatial pattern of amplified surface current. An example from Dr Thomas Schlick (*personal communication*, 2006) is shown in Fig. 5 for the 26 December 2004 tsunami in the Indian Ocean as it approached the Seychelles. The Bureau of Meteorology run the same model (MOST) for tsunami work and have developed a scenario database for simulated tsunamis occurring at 100 km intervals along the subduction zone through NZ up to PNG. Each source location has 4 scenarios associated

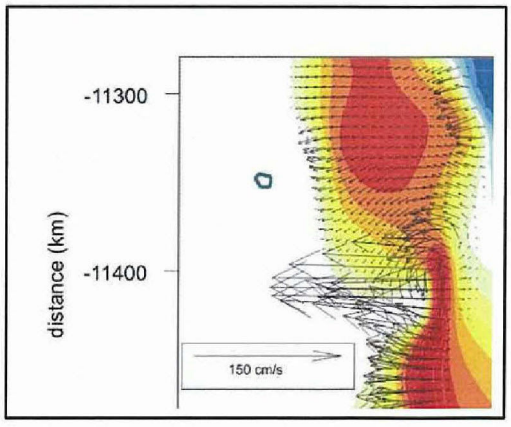

Figure 5. Surface current vectors calculated using the MOST hydrodynamic model for the edge of the continental shelf on the eastern side of the Seychelles plateau. The driving conditions emulate those of the 26 December 2004 tsunami. The shaded contours refer to water elevation (which we do not use) and the arrows indicate the amplification of surface currents by HF radar (Thomas Schlick, University of Hamburg)

with it, with moment magnitudes of 7.5, 8, 8.5 and 9 (Greenslade et al., 2007). In this project we are running the MOST model for a set of scenarios like this to estimate the surface current amplification patterns at the edge of the continental shelf near Heron Island. This will provide a set of reference current maps to use when we are detecting small tsunamis. The surface current maps will be grouped into a basis set of surface current responses and these will form reference patterns for analysis of the radar data. The radial component in the direction of the Tannum Sands radar and the Lady Elliot Island radar will be calculated for each reference pattern. Pattern recognition techniques will be developed to compare these patterns with actual radar-observed radial current maps and determine the threshold of detection. This approach has a huge advantage over analysing surface currents in individual pixels because the advantage in coherent detection over many pixels. It is anticipated that this approach will identify small, non-destructive tsunamis. The potential for this work is to examine the causal link between the seismic origin and the eventual tsunami produced by each event.

5. Summary

The HF coastal ocean surface radar over the Capricorn and Bunker Groups is set to make a huge impact on the understanding of shelf dynamics by contributing quality data on surface currents, waves and winds into the IMOS national archive.

6. Acknowledgements

The GBR HF radar was acquired under Australian Research Council Grant LE0560892 with partner institutions James Cook University, The University of Queensland, The Australian Institute of Marine Science, and the National Oceanic and Atmospheric Administration, USA. It will become an operational part of the Australian Coastal Ocean Radar Network (ACORN) for data quality assurance and archiving. The hydrodynamic modeling project is supported by ARC Grant LP0562157; the other projects form part of an ARC proposal for 2008. The manuscript contents are solely the opinions of the authors and do not constitute a statement of policy, decision, or position on behalf of NOAA or the U.S. Government.

7. References

Arzayus, L.F. and W.J.Skirving, (2004) The correlation between ENSO and coral bleaching events, 10th International Coral Reef Symp., Okinawa, Japan.

Barrick, D.E., (1972) Remote sensing of sea state by radar, In *Remote Sensing of the Troposphere,* ed. V.E.Derr, U.S. Govt. Printing Office, Washington, DC

Barrick, D.E. 1977 Extraction of wave parameters from measured HF sea echo Doppler spectra, Radio Science, 12, 415-424.

Barrick, D.E, (1979) A coastal radar system for tsunami warning, Remote Sensing of the Environment, 8, 353-358.

Bryant, E., (2001) Tsunami: the underrated Hazard, Cambridge University Press, 320pp.

Crombie, D.D., (1955) Doppler spectrum of sea echo at 13.56 Mc/s, Nature, 175, 681-682.

de Silva Samarasinghe, J.R., (1989) Transient salt-wedges in a tidal gulf: A criterion for their formation. Estuarine, Coastal and Shelf Science, **28**, 129-148.

Gerlach, G., J.Atema, M.J.Kingsford, K.P.Black and V. Miller-Sims, (2007) Smelling home can prevent dispersal of reef fish larvae, PNAS, doi:10.1073/pnas.0606777104.

Graber, H.C. and M.L.Heron, (1997) Wave height measurements from HF radar, Oceanogr., 10, 90-92.

Greenslade, D.J.M., M.A.Simanjuntak, D.Burbidge and J.Chittleborough, (2007) A first-generation real-time tsunami forecasting system for the Australian Region, BMRC Report No 126, Bur. Met. Australia.

Hearn, C.J., (1985) On the value of the mixing efficiency in the Simpson-Hunter h/u^3 criterion. D. Hydrographisches Zeitschrift, **38(H.3)**, 133-145.

Heron, S.F. and M.L. Heron (1998) A comparison of algorithms for extracting significant wave height from HF radar ocean backscatter spectra, *J. Atmospheric and Oceanic Technology*, 15, 1157-1163.

Heron, M.L. and A.Prytz, (2002) Wave height and wind direction from the HF Coastal Ocean Surface Radar, Can. J. Remote Sensing, **28**, 385-393.

Mao, Y and M.L.Heron (2007) The influence of fetch on the response of surface current to wind, J. Phys. Oceanography, submitted.

Mao, Y., M.L. Heron and P.V. Ridd, (2007) Empirical modeling for search and rescue operations, IEAust. Coasts and Ports Conference, Melbourne

Prytz, A. and M.L. Heron (1999) On the flushing of Port Phillip Bay, J. Mar. Freshw. Res., 50,483-492.

Sammarco, P.W. (1994), Larval dispersal and recruitment processes in Great Barrier Reef corals: Analysis and synthesis. *In P.W.Sammarco and M.L.Heron (eds.), The Bio-Physics of Marine Larval Dispersal, Am. Geophys. Union, Wash. DC*, pp35-72.

Sammarco, P.W. and J.C. Andrews. 1988. Localized dispersal and recruitment in Great Barrier Reef corals: The Helix Experiment. Science 239: 1422-1424.

Sammarco, P.W. and J.C. Andrews. 1989. The Helix Experiment: Differential localized dispersal and recruitment patterns in Great Barrier Reef corals. Limnol. Oceanogr. 34: 896-912.

Skirving W.J., M.L.Heron and S.F.Heron, The hydrodynamics of a bleaching event: Implications for management and monitoring, *in Coral Reefs and Climate Change: Science and Management* Eds: Jonathan T. Phinney, William J. Skirving, Joanie Kleypas, Ove Hoegh-Guldberg, Alan E. Strong, Coastal and Estuarine Series, Volume 61, 2006, 350 pp, ISBN 0-87590-359-2, AGU Code: CE0613592

Simpson, J.H. and Hunter, J., Fronts in the Irish Sea. Nature, **250**, 404-406, 1974

Smith, W.H.F., R.Scharroo, V.V.Titov, D.Arcas and B.K.Arbic, 2005 Satellite altimeters measure tsunami, Oceanography, 18(2), 11-13.

Wyatt, L.R. and G.J. Holden (1994), HF radar measurement of multimodal directional wave spectra. *Global Atmosphere and Ocean System,* 2, 265-290.